State-selective dielectronic-recombination measurements for He- and Li-like carbon and oxygen ions

Lars H. Andersen, Jakob Bolko, and Poul Kvistgaard
Institute of Physics, University of Aarhus, DK-8000 Aarhus C, Denmark
(Received 10 July 1989)

Dielectronic recombination due to the $2s \rightarrow 2p$ excitation has been measured for metastable He-like C^{4+} and O^{6+} ions and for Li-like C^{3+} and O^{5+} ions. The measurements have been performed with a merged-beams technique. An energy resolution of 0.135 eV was obtained. The data for the Li-like ions are compared with distorted-wave calculations. For the low-lying resonances, good agreement is found between experiment and theory except for one resonance ($2p4l$) for C^{3+} that is very close to threshold. The contribution due to higher Rydberg states is in agreement with theory for external fields of 3 V/cm for C^{3+} and around 7 V/cm for O^{5+}. The field present in the experiment is expected to be around 2 V/cm. Large and unexpected structures are observed in the He-like data. These have tentatively been explained in terms of interaction between different core configurations. For the metastable He-like ions extremely large cross sections of the order of 10^{-15} to 10^{-14} cm^2 are found.

I. INTRODUCTION

When a free electron and an ion are to combine, excess energy and momentum have to be given away to some third "particle." In the process of radiative recombination,[1,2] the excess energy provides the creation of one or more photons. Radiative recombination is a nonresonant process with relatively small cross sections. Therefore cross sections for this process have not yet been obtained experimentally. When the density of electrons is sufficiently high and the temperature of the electrons sufficiently low, the energy may also be taken up by another free electron. This process is known as collisional recombination.[3] In the present paper, we report on the dielectronic-recombination (DR) processes, in which the excess energy is given to a core electron of the ion which then becomes excited. The originally free electron becomes bound to some state nl of the ion. If the doubly excited state decays by photon emission, the dielectronic-recombination process is completed. If not, elastic scattering has occurred. The DR process is resonant and normally associated with cross sections of the order of $10^{17}-10^{-18}$ cm^2. It is therefore easier to measure than the process of radiative recombination, which is associated with much smaller cross sections.

If the free electron is associated with the kinetic energy E_r relative to the ion, and the core-excitation energy is ΔE, then for the state nl energy conservation yields

$$E_{nl}+E_r=\Delta E \ , \tag{1}$$

where E_{nl} is the binding energy of the state nl. When ΔE is small compared to the total binding energy of the core electron, high Rydberg states (nl) are populated. The core-excitation ΔE is then normally unaffected by the presence of the Rydberg electron which merely acts as a spectator. As will be discussed below, however, the Rydberg electron may play a very important role when different core configurations can mix. This happens in particular when core (1)nl states are energy degenerate with core (2)$n'l'$ states.

Here we report dielectronic-recombination measurements with metastable He-like C^{4+} and O^{6+} ions. The following reactions were considered:

$$e^- + A^{q+}(1s2s\ ^1S) \rightarrow A^{(q-1)+}(1s2p\ ^1Pnl) \tag{2}$$

$$\rightarrow A^{(q-1)+}(1s2p\ ^3Pnl) \ , \tag{3}$$

$$e^- + A^{q+}(1s2s\ ^3S) \rightarrow A^{(q-1)+}(1s2s\ ^1Snl) \tag{4}$$

$$\rightarrow A^{(q-1)+}(1s2p\ ^3Pnl) \tag{5}$$

$$\rightarrow A^{(q-1)+}(1s2p\ ^1Pnl) \ , \tag{6}$$

where A^{q+} is either C^{4+} or O^{6+}. As will be seen from the present results, the DR cross sections related to these transitions are extremely large. In an earlier paper,[4] we reported on DR measurements for O^{6+} ions. For convenience, these data will be presented again, together with improved measurements with O^{6+}.

We also present data obtained with Li-like ions of C^{3+} and O^{5+}. Here the DR process is related to the following reaction:

$$e^- + A^{q+}(1s^22s) \rightarrow A^{(q-1)+}(1s^22pnl) \ , \tag{7}$$

where A^{q+} is either C^{3+} or O^{5+}. These systems have been considered before both experimentally[5,6] and theoretically.[7-11]

To reveal the resonant structure of the dielectronic-recombination process, sources of electrons with good energy definition are needed. In the present work, the spread in relative energy is as low as 0.135 eV, which is more than a factor of 30 better than that obtained in previous merged-beams measurements.[12] Consequently, the present data provide a more severe test of the calculations on DR.

The present data have been obtained with a so-called electron cooler. Electron cooling is one scheme for reduction of the beam phase space in storage rings.[13] When a beam of electrons with little momentum spread (i.e., cold electrons) is merged with stored ions, cooling of the ions will take place due to the mutual Coulomb interaction; transverse momentum is transferred from the ions to the electrons. The apparatus was built to serve two purposes. First, it provides an ideal target of electrons with well-defined energy. Second, the apparatus was built as a prototype for the electron cooler at the heavy-ion storage ring at the University of Aarhus.[14]

II. EXPERIMENTAL TECHNIQUE

The present results have been obtained with merging beams of electrons and ions. Figure 1 shows the experimental setup schematically. The ion beams were provided by the 6-MV EN tandem accelerator at the University of Aarhus. The C^{3+}, C^{4+}, and O^{5+} beams were extracted directly from the terminal of the machine, whereas O^{6+} was produced by a thin post-stripper foil. Immediately in front of the interaction region, the beam was cleaned for unwanted charge-state components by a 15° bending magnet. After the 1 m interaction region, the ions were charge-state-analyzed by an electric field perpendicular to the beam direction. This field sets an upper limit $n_{\max}$ for the main quantum number of states which survive through the analyzer according to

$$n_{\max}=(6.2\times10^{8}\ q^{3}/E)^{1/4}\ , \tag{8}$$

where E is the electric field strength in V/cm (Ref. 15). Fields in the order of 10 kV/cm were applied. Finally, the main beam was collected in a Faraday cup, and the small fraction of ions, which had captured an electron either from rest-gas molecules in the vacuum system or from the electron beam, was detected by a position-sensitive channel-plate detector. Two quadrupole doublets were used to guide the ion beam through the setup. The alternative method of using slits to define the beam path was avoided in order not to create slit-edge-scattered particles and to maintain the high ion flux through the interaction region. The ion-beam current was typically 1 μA.

As mentioned above, electron capture from the rest gas constitutes a background signal. Therefore, great efforts were used to keep the pressure as low as possible. With both ion and electron beam on, the pressure in the interaction region was about 2×10^{11} torr. The rest-gas composition was dominated by H_2. At the largest DR resonances, the signal-to-background ratio was about 10:1.

The electrons were accelerated in an electron gun with Pierce geometry,[16] see Fig. 1. The gun produced an electron beam with a diameter of 1 cm. It was verified with a Faraday probe that the intensity variation of the electron beam, within a diameter of 0.8 cm, was less than 5%. Figure 2 shows the profile of the electron beam at 1000 eV.

The electron current was space-charge limited, and it was in terms of the acceleration voltage V_c given by $I_e=PV_c^{3/2}$. The perveance P could be changed by varying the distance between the cathode and the gridded anode. P was typically $\approx5\times10^{-7}$ (A/V$^{3/2}$), yielding electron currents of about 10 mA in the present experiment with MeV/amu ion beams. Three solenoids and two toroids guided the electrons from the gun through the interaction region to the collector. The magnetic field of 100–200 G, depending on electron energy, was applied to compensate for the space-charge field in the electron beam. Care was taken to make a homogeneous magnetic field in the electron beam. Figure 3 shows the variation of the field strength along the center path of the electrons from the gun to the collector. On the three straight sections of the electron path, dipole magnets were used to slightly steer the electron beam.

We were able to modulate the anode voltage by 2.5 V at a frequency of 2 MHz, and the electron-beam intensity was modulated accordingly. The horizontal and vertical

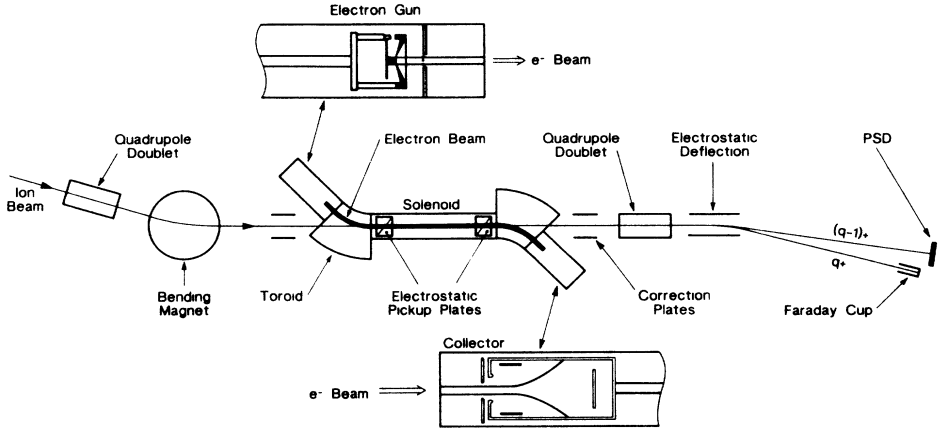

FIG. 1. Schematic diagram of the experimental setup.

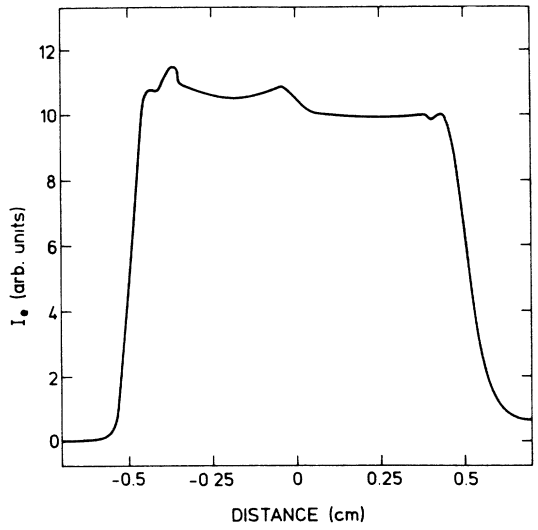

FIG. 2. Electron-beam profile at the exit of the merge region. The electron energy is 1000 eV.

positions of the electron beam in the merge section was then measured via the voltage induced on two oppositely mounted electrostatic pickup plates. The buncher facility of the tandem accelerator was used to modulate the ion-beam intensity at the same frequency to monitor the ion-beam position in the merge region. In this way, the overlap between the two beams was known since the ion beam was fully embedded in the electron beam, the diameter of which was larger than that of the ion beam (see also Fig. 4).

The actual energy of the electrons was given by the formula (in the laboratory frame)

$$E_e=(V_c+V_s)e \ , \tag{9}$$

where V_s is the space-charge potential in the electron beam and e is the elementary charge. The space-charge potential varies slightly across the electron beam, causing a small longitudinal spread in the electron energy. With the present geometry, we calculate

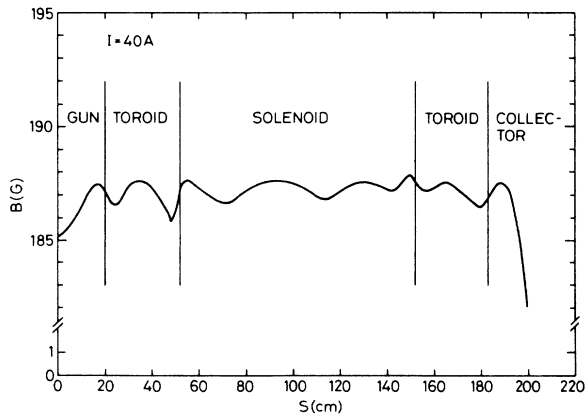

FIG. 3. The variation of the magnetic field along the center line of the electron beam.

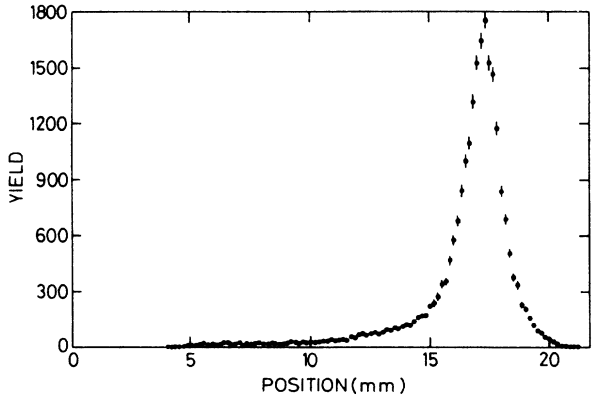

FIG. 4. The ion-beam profile as detected on the position-sensitive channel-plate detector. The ion beam $N^{(q-1)+}$ is 20-MeV O^{4+}.

$$V_s=-K(r)\frac{I_e}{\sqrt{E_e}} \tag{10}$$

with I_e in mA and E_e in eV. At the center of the electron beam, $K(r=0)=85$ V and on the edge $K(r=r_0)=78$ V. In the rest frame of the ion, the energy of the electron E_r was obtained as

$$|E_r|=E_e+\frac{m}{M}E_i-2\left[E_iE_e\frac{m}{M}\right]^{1/2} \ , \tag{11}$$

where E_i is the ion energy and m and M are the electron mass and ion mass, respectively. We used the convention that negative E_r corresponds to $v_e<v_i$ and positive E_r corresponds to $v_e>v_i$, where v_e and v_i are the electron and the ion velocity, respectively. We found the DR resonances to lie symmetrically with respect to $E_r=0$ for values of K very close to 85 V, implying that there was little space-charge neutralization due to trapped positive ions in the interaction region.

Let N^{q+} be the number of incoming ions with charge q^+ collected in the Faraday cup and $N^{(q-1)+}$ the number of ions with charge $(q-1)+$ detected in the position-sensitive detector. Figure 4 displays the beam profile at the ion detector. Then, in the measurement, we recorded the number of ions $N^{(q-1)+}$ on the channel plate as a function of the relative energy of the electrons given by Eq. (11). Figure 5 shows such a spectrum for incoming O^{5+}. Evidently, there is a large nonresonant background contribution, on top of which is the resonant DR signal. A second-order polynomial was fitted to this contribution in energy regions where no DR resonances were present. We then subtracted this background $N_0^{(q-1)+}$ from the spectrum and obtained the true DR signal.

We choose to represent our data in the form of the rate coefficient defined as

$$\langle v\sigma\rangle=\frac{1}{\epsilon}\frac{N^{(q-1)+}-N_0^{(q-1)+}}{N^{q+}}\frac{v_i}{\rho_eL} \ , \tag{12}$$

where v is the electron velocity in the ion frame, ρ_e is the

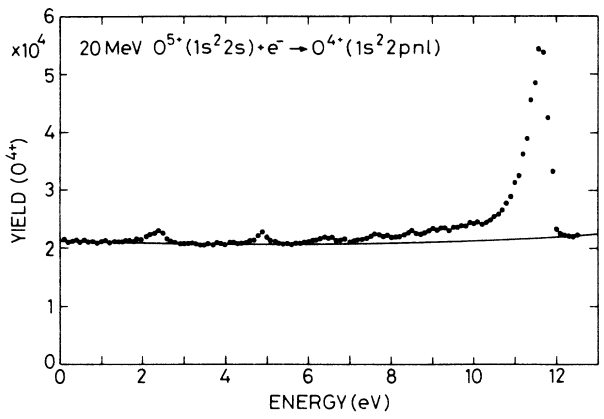

FIG. 5. $N^{(q-1)+}$ as a function of relative energy for 20-MeV $O^{5+}+e^- \rightarrow O^{4+}$. The solid line is the fit to the nonresonant background contribution $N_0^{(q-1)+}$.

electron density, and L is the interaction length. ϵ, the ion-detection efficiency, was measured directly by comparing count rates in the channel plate and in a solid-state detector mounted permanently in the vacuum system. We found $\epsilon=80\%\pm5\%$ for the C beams and $\epsilon=90\%\pm5\%$ for the O beams. The combined uncertainty of $\langle v\sigma\rangle$ is estimated to be $\pm20\%$. This includes uncertainties due to the beam current measurements, the ion-beam–electron-beam overlap, the effective target length, and background subtraction.

To be able to compare the experimentally obtained rate coefficient Eq. (12) with theory, the electron-velocity distribution $f(\mathbf{v})$, as seen in the rest frame of the ion, must be known. The relation between the cross section σ and the rate coefficient is

$$\langle v\sigma\rangle=\int\sigma(v)vf(\mathbf{v})d\mathbf{v}\ . \tag{13}$$

We choose to write $f(\mathbf{v})$ as a product of two Maxwell distributions,

$$f(\mathbf{v})=\frac{m}{2\pi kT_\perp}e^{-mv_\perp^2/2kT_\perp} \times\left[\frac{m}{2\pi kT_\parallel}\right]^{1/2}e^{-m(v_\parallel-\Delta)^2/2kT_\parallel}\ , \tag{14}$$

where $v_\perp$ and $v_\parallel$ are the electron-velocity components perpendicular and parallel to the ion beam, respectively, and Δ is the detuning velocity given by $\frac{1}{2}m\Delta^2=E_r$. $T_\perp$ and $T_\parallel$ are the two temperatures which characterize the relative motion of the electrons and ions. To obtain values for $kT_\perp$ and $kT_\parallel$, we utilized the fact that the DR cross section for a single resonance is narrow and represented the cross section by a δ function. Figure 6 shows the resulting rate coefficient for an artificial resonance at the relative energy of 0.15 eV. Evidently, the resulting shape of the rate coefficient as a function of energy is very sensitive to the two "temperatures" $kT_\perp$ and $kT_\parallel$. It is seen that the curve towards low energies is sensitive to $kT_\perp$, and the curve towards higher energies is sensitive to $kT_\parallel$. This allows for an independent determination of $kT_\perp$ and $kT_\parallel$. Figure 7 shows a fit to the $1s2s(^1S)\rightarrow1s2p(^1P)11l$ DR resonance of O^{6+} (to be discussed later). Evidently, the distribution function Eq. (14) describes the measured resonance well. From fits to several resonances, we obtained $kT_\perp=0.135\pm0.010$ eV and $kT_\parallel=(10\pm5)\times10^{-4}$ eV for the two temperatures.

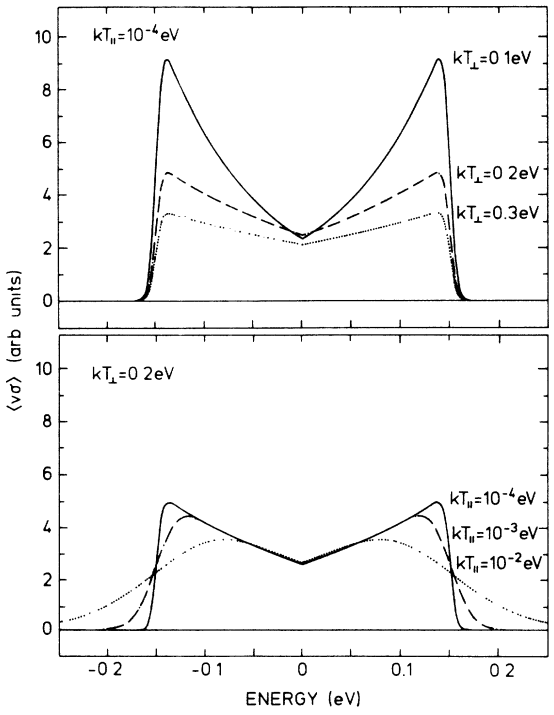

FIG. 6. Artificial DR resonance generated for different electron temperatures. Upper figure ($kT_\parallel=10^{-4}$ eV): · · · ·, $kT_\perp=0.3$ eV; —·—·—·, $kT_\perp=0.2$ eV; ——, $kT_\perp=0.1$ eV. Lower figure ($kT_\perp=0.2$ ev): · · · ·, $kT_\parallel=10^{-2}$ eV; —·—·—·, $kT_\parallel=10^{-3}$ eV; ——, $kT_\parallel=10^{-4}$ eV.

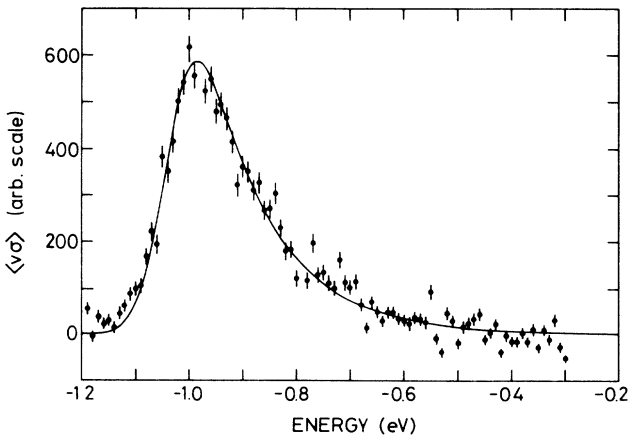

FIG. 7. Fit to the O^{6+} $[1s2s(^1S)]+e^-\rightarrow O^{5+}[1s2p(^1P)11l]$ DR resonance. The solid curve results when $\sigma(v)$ is a δ function, and the rate coefficient is given by Eqs. (12) and (13).

As expected, due to the kinematic reduction of the longitudinal energy spread, $kT_{\parallel} \ll kT_{\perp}$. There is no kinematic reduction of the transverse energy spread. $kT_{\perp}$ is found to be about 50% larger then expected from a cathode at the temperature of 1000 K. Additional heating may take place during the transport of the electrons through the anode and in the magnetic field in the interaction region. It should be emphasized that the use of a δ function to describe the resonance is idealistic. If several resonances with different l-quantum numbers in fact contribute to the DR process over a nonnegligible energy range, the temperatures obtained are overestimated. Thus the obtained values are to be considered as upper limits.

III. RESULTS AND DISCUSSION

A. He-like ions

The excitation energy of the $1s^2(^1S) \rightarrow 1s2p(^1P)$ transition is 308 eV for C^{4+} and 574 eV for O^{6+}. In the energy range used in the present investigation (0→14 eV), there are no DR resonances related to this excitation. Hence the observed DR resonances with C^{4+} and O^{6+} have to be due to metastable states. The lifetimes of the $1s2s(^1S)$ and $1s2s(^3S)$ states are longer than or comparable to the flight time from the place of production to the region where the beams merge. We do not know the exact fractions of metastables in the ion beam, and in that sense, the data give information only on the relative cross sections. When applying Eq. (12) to determine $\langle v\sigma \rangle$, we simply used the total number of ions in any state as N^{q+}. Thus the rates obtained with the metastable He-like ions are to be considered as lower limits. The fraction of metastable ^3S states in the ion beam is likely to be in the order of 30%.[17] Assuming a statistical population $(2S+1)$ of the ^1S and ^3S states, the initial population of the ^1S state is in the order of 10%. Due to the relatively short lifetime of the ^1S state,[18] only 5–10 % will live long enough to reach the electron target. Thus a rough estimate of the state population at the target is $1s^2(^1S)$, 70%, $1s2s(^3S)$, 30%; and $1s2s(^1S)$, $\leq 1\%$. The rate coefficient associated with the $^1S \rightarrow {}^1P$ excitation may therefore be 100 times larger than the values quoted here.

For convenience, we show in Fig. 8 a schematic level diagram with the possible core excitations of the two metastable states $1s2s(^1S)$ and $1s2s(^3S)$ indicated. As seen in the figure, there are up to five different excitations for the He-like ions. The DR resonances are expected at relative energies according to

$$E_n = \Delta E - \frac{q^2 13.6}{n^2} , \tag{15}$$

where ΔE is the core-excitation energy related to one of the five possible excitations. In the present work, we obtained these energies from calculations of Drake.[19] In Eq. (15) we neglected the quantum defect. Consequently, DR resonances with low-to-medium n quantum numbers may be found at a slightly lower energy than given by Eq. (15). Moreover, Eq. (15) does not predict the positions of the different angular-momentum states.

Figure 9 presents the experimental results for C^{4+}. The figure shows the expected positions of the DR resonances according to Eq. (15). It is seen that the signal related to the $1s2s(^1S) \rightarrow 1s2p(^1P)$ excitation dominates, even though the metastable fraction for this initial state may be as low as 1%. This is due to the strong radiative stabilization of the doubly excited intermediate state,

$$1s2p(^1P)nl \rightarrow 1s^2(^1S)nl + h\nu . \tag{16}$$

Taking into account the small fraction of ^1S states in the ion beam, we obtain DR cross sections in the order of 10^{-15} to 10^{-14} cm^2, which are much larger than for any other system studied so far. This experimental finding is consistent with recent theoretical calculations.[20,21]

In C^{4+}, the $1s2s(^1S)$ and $1s2p(^3P)$ core states are almost energy degenerated. The $1s2p(^3P)$ state lies just above the $1s2s(^1S)$ state, the energy difference being only 0.008 eV. Thus, in principle, dielectronic recombination involving very high Rydberg states is possible for the $^1S \rightarrow {}^3P$ excitation. According to Eq. (15), n should then be larger than about 160. Such high Rydberg states are ionized in the analyzer field, and consequently, this DR

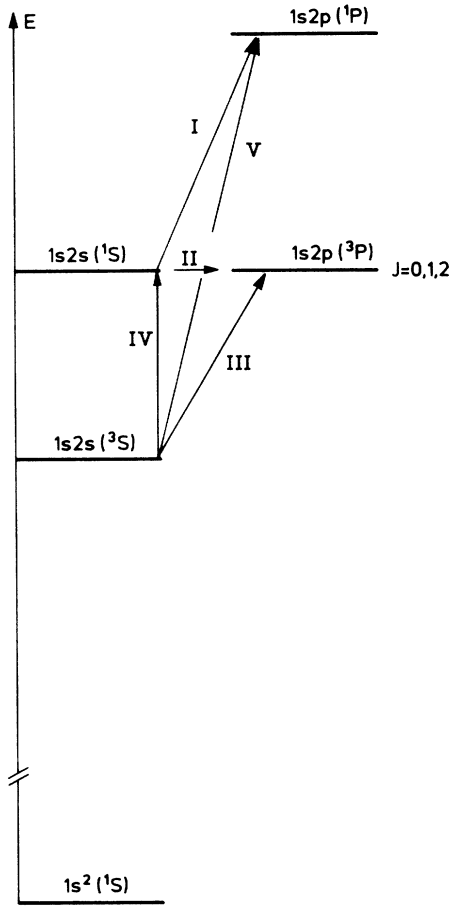

FIG. 8. Schematic level diagram of the $1s2s$ and $1s2p$ states of C^{4+} and O^{6+}.

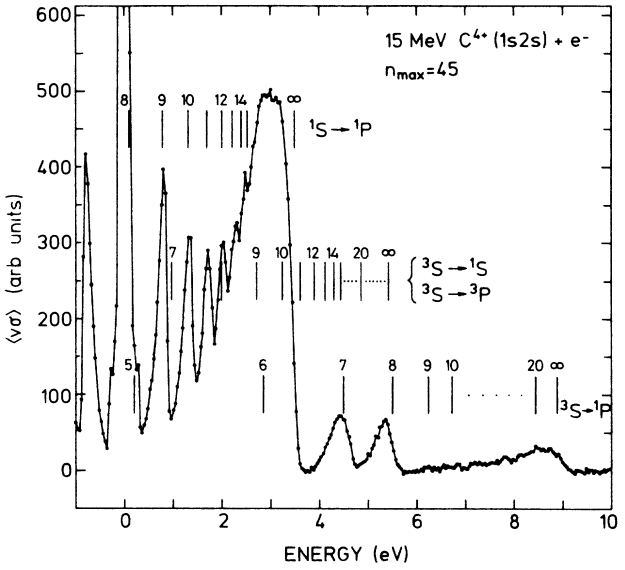

FIG. 9. Dielectronic-recombination rate coefficient $\langle v\sigma \rangle$ as a function of energy for 15-MeV C^{4+}. To obtain a lower limit of the rate coefficient, multiply the ordinate by 10^{-12} cm^3/s.

process will not be observed. By varying the place of production of the C^{4+} ions (terminal, post-stripper foil), it was verified that the very intensive peak at zero energy (see Fig. 10) was due to excitation of the ^1S core state.

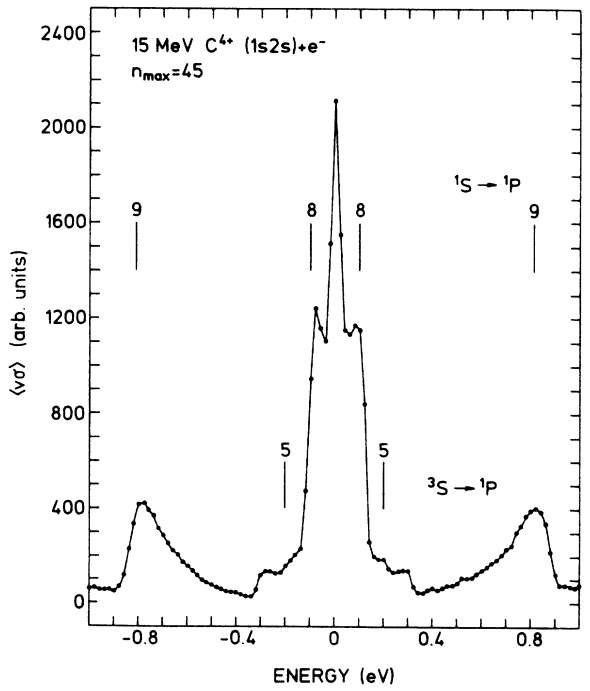

FIG. 10. DR spectrum for 15-MeV C^{4+} for relative energies between -1 and 1 eV. To obtain a lower limit of the rate coefficient, multiply the ordinate by 10^{-12} cm^3/s.

Most likely, it is due to members of the $n=8$ resonance of the $^1S \rightarrow {}^1P$ transition.

The rate coefficient for radiative-recombination peaks at zero energy. Our calculations, however, show that the rate coefficient is only about 5×10^{-11} cm^3/s at zero energy with the present electron temperatures. Moreover, the observed sharp peak cannot be due to radiative recombination because of the weak energy dependence of the cross section of this process.

For the ^3S initial core state, three excitations (III–V) are possible. It is immediately seen that these series are weaker than the strong $^1S \rightarrow {}^1P$ series (I), and mainly only the series limits (large n values) are recognized in the data. The two transitions $^3S \rightarrow {}^1S$ and $^3S \rightarrow {}^3P$ (III and IV) appear as only one series due to the small energy difference. In Fig. 10 are seen small resonances which may be due to $n=5$ for the $^3S \rightarrow {}^1P$ excitation.

The large peak at around 4.5 eV appears where the $n=7$ resonance of the $^3S \rightarrow {}^1P$ series nearly coincides with the $n=14$ and 15 resonances of the $^3S \rightarrow {}^1S$, ^3P series. Extraordinarily large DR signals have been observed for He-like O^{6+} (Ref. 4) (see the data presented below) and have been interpreted as being due to configuration interaction (CI).[22] The near degeneracy of the states will cause them to interact so that the different core configurations mix. In the present case this means that the ^1S and ^3P cores mix with the ^1P core. Since the ^1P core very quickly makes the radiative transition to the core ground state [Eq. (16)], an enhanced DR signal results. Theoretically, the effect of the configuration interaction has been considered before,[11,23] but the present data may provide the first experimental evidence for the importance of configuration interaction in DR processes.

Figures 11 and 12 show the data obtained with He-like O^{6+}. As for C^{4+}, the series associated with the $^1S \rightarrow {}^1P$ core excitation is dominating. Close to zero energy, a very strong resonance is observed. This is due to $n=10$ of the $^1S \rightarrow {}^1P$ excitation and possibly due to $n=8$ of the $^3S \rightarrow {}^1S$ excitation. The very sharp peak right at zero energy cannot be due to radiative recombination. It is too large and narrow. According to the energy calculations,[19] the ^3P level lies below the ^1S level, and consequently, transition II is not possible for O^{6+}. The energy difference between the ^1S and ^3P levels is 0.24 eV, and therefore two distinguishable series ($^3S \rightarrow {}^3P$ and $^3S \rightarrow {}^1S$) should emerge. From the position of the observed Rydberg series limit, it appears that the $^3S \rightarrow {}^3P$ reaction is the more dominant. The Rydberg series limit of the $^3S \rightarrow {}^1P$ excitation at 12.9 eV is also seen although it is weaker than the other series. As reported earlier,[4,22] there may be effects of configuration interaction in the O^{6+} spectrum. This appears at about 2.5, 4.4, and 6.5 eV, where unusually large rates are observed. It may be caused by CI between the $n=7$, 8, and 9 members of the $^3S \rightarrow {}^1P$ series with several (n) members of the $^3S \rightarrow {}^3P$ and $^3S \rightarrow {}^1S$ series.

Thus, the effect of CI below the ^1S and ^3P series limit is an increase in the cross section at energies where certain energy levels match in energy. Above these series limits CI will tend to decrease the cross section due to the open Auger channel to the ^1S and ^3P core states.[22]

B. Li-like data

In Fig. 13 is shown the DR spectrum obtained with $C^{3+}(1s^2 2s)$. The data exhibit a strong Rydberg series that terminates at a relative energy of 8 eV which is the $2s \rightarrow 2p$ excitation energy. At lower energies, resonances are observed which are due to capture to the $n \geq 4$ levels. The data are compared with distorted-wave calculations.[9]

The theoretical cross sections were integrated over small energy bins to yield an energy averaged cross section $\bar{\sigma}$,

$$\bar{\sigma}_{\epsilon_0} = \frac{1}{\Delta\epsilon} \int_{\epsilon_0 - \Delta\epsilon/2}^{\epsilon_0 + \Delta\epsilon/2} \sigma(\epsilon) d\epsilon \ , \tag{17}$$

where $\Delta\epsilon$ is the energy-bin size of 0.0005 hartrees. To obtain the rate coefficient for comparison with the data, we calculated

$$\langle v\sigma \rangle = \int_0^\infty \sigma(E) \left[\frac{2E}{m} \right]^{1/2} \frac{dN}{dE}(E) dE$$

$$= \sum_i \bar{\sigma}_{\epsilon_0^i} \int_{(i-1)\Delta\epsilon}^{i\Delta\epsilon} \left[\frac{2E}{m} \right]^{1/2} \frac{dN}{dE}(E) dE \ , \tag{18}$$

where the density dN/dE is given as

$$\frac{dN}{dE} = \frac{V}{m} \int_\Omega f(\mathbf{v}) d\Omega \ , \tag{19}$$

with $f(\mathbf{v})$ defined in Eq. (14). We used $kT_\parallel = 10^{-3}$ eV and $kT_\perp = 0.135$ eV.

The distorted-wave calculation[9] was performed with different electric fields in the interaction region. The

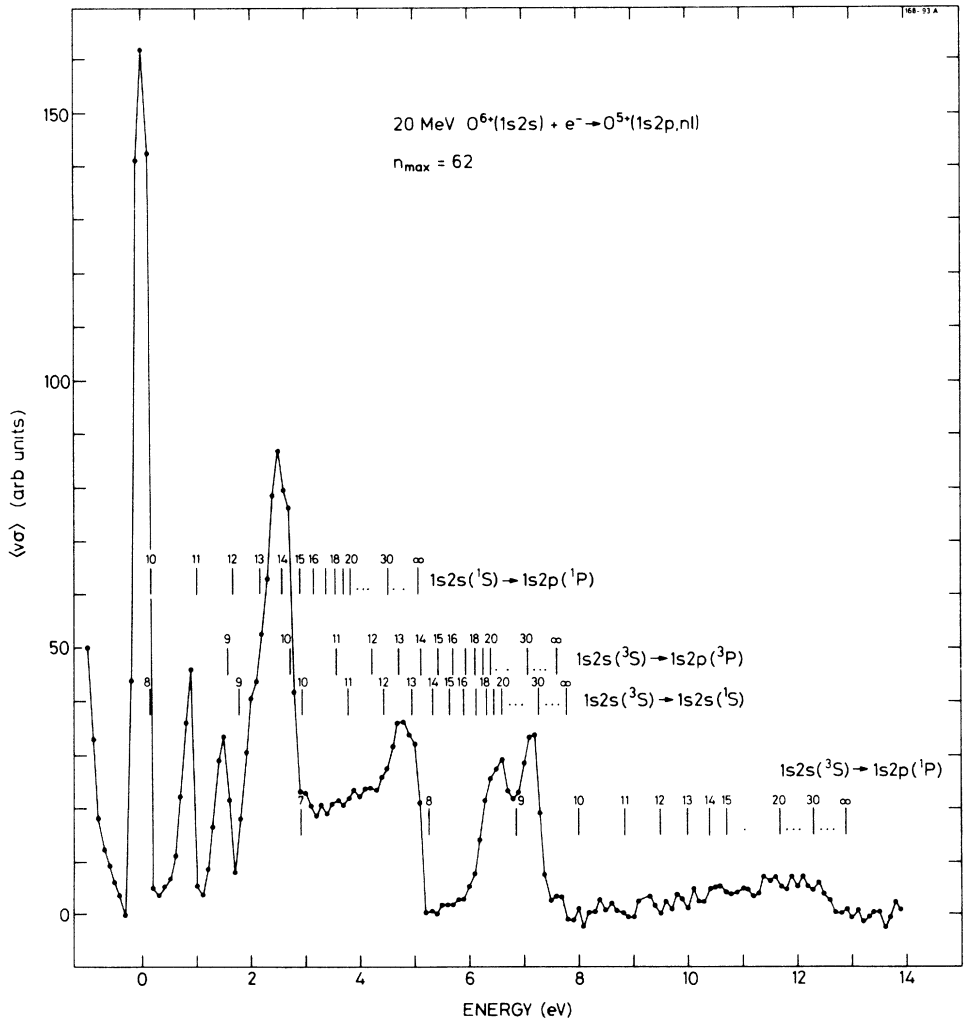

FIG. 11. Dielectronic-recombination rate coefficient $\langle v\sigma \rangle$ as a function of energy for 20-MeV O^{6+}. To obtain a lower limit of the rate coefficient, multiply the ordinate by 10^{-11} cm^3/s.

electric field, perpendicular to the beam direction, is due to the space-charge potential. The DR cross section is sensitive to such static electric fields because it results in a mixing between the different angular-momentum states l of a given Rydberg state. The net effect is an increase in the cross section because more l states contribute to the DR process.[24]

Evidently, experiment and theory are in agreement for a field of about 3 V/cm. In order to estimate the actual field in the merge region, we recorded the ion-beam profile with the Faraday probe in the merge section. It was found to be approximately Gaussian, with a width of 2mm (2σ). The average electric field is then calculated to be 1.8 V/cm.

Earlier measurements with C^{3+} (Ref. 6) indicated that the theory underestimates the DR cross section involving Rydberg states. The present data confirm that trend.

There seems to be a slight disagreement between theory and experiment about the resonance positions for the $n=5$, 6, and 7 resonances. These shifts are not understood. Apparently, the Rydberg peak is measured at the expected position.

The low-energy part of the DR spectrum for C^{3+} is shown in Fig. 14. The disagreement with theory of about a factor of 2 for the $n=4$ resonances is not due to an incorrectly assumed field because the $1s^2 2p 4l$ intermediate resonances is basically unaffected by the present external field. The cross section, however, is very sensitive to the energy of the levels employed in the calculation so close to threshold.[9] The discrepancy may also be due to the neglect of the $n=4$ electron in the calculation of the $2s \rightarrow 2p$ radiative transition.

The data obtained with the Li-like O^{5+} ions are presented in Fig. 15. Here the Rydberg series limit is at 12 eV corresponding to the $2s \rightarrow 2p$ core-excitation energy in O^{5+}. The data are compared to the distorted-wave calculation.[9] The low-energy resonances ($n=6$–8) are in good agreement with theory. At higher energies, the theory seems to underestimate the DR cross section, especially if the field is as low as 2 V/cm. If the ion beam

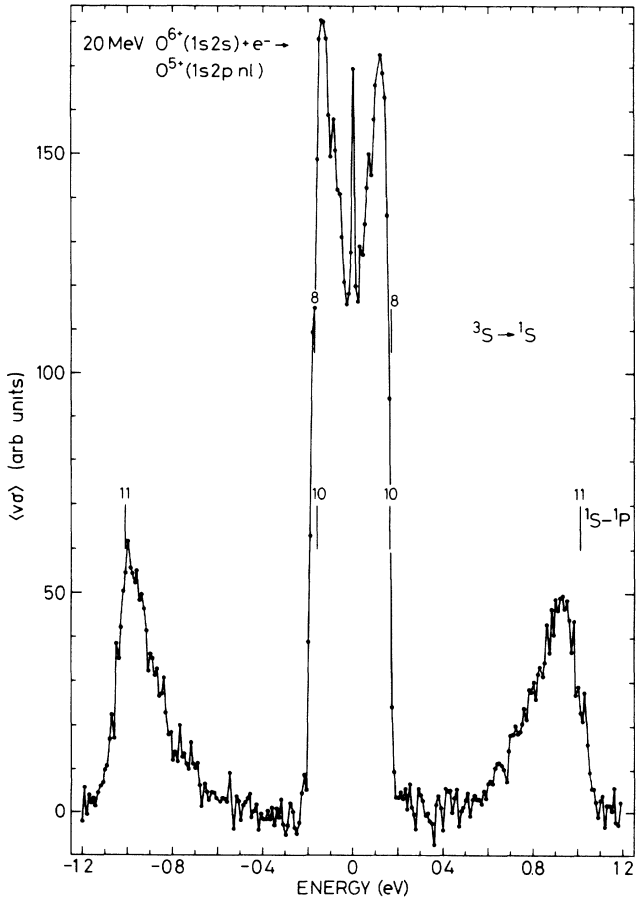

FIG. 12. DR spectrum for 20-MeV O^{6+} for relative energies between -1 and 1 eV. To obtain a lower limit of the rate coefficient, multiply the ordinate by 10^{-11} cm^3/s.

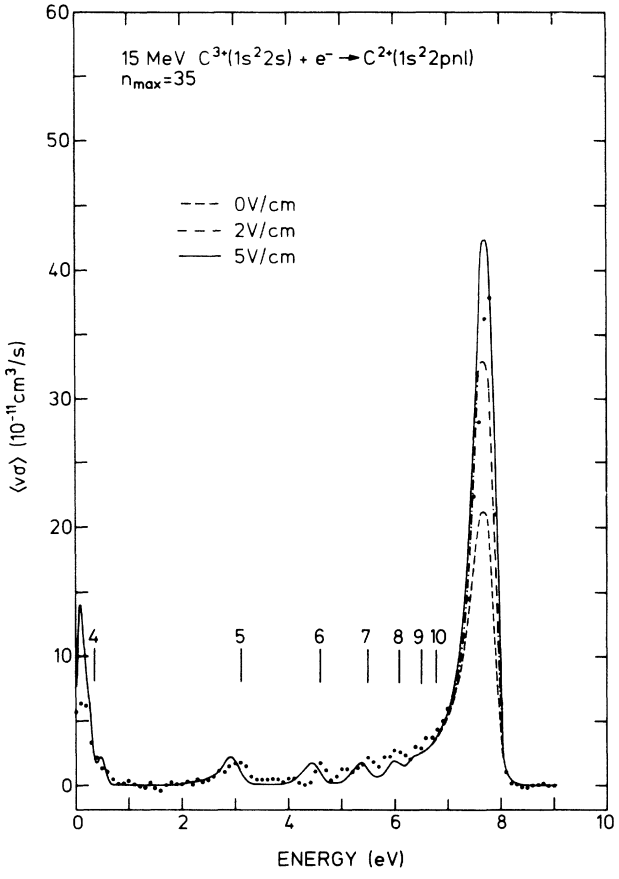

FIG. 13. Dielectronic-recombination rate coefficient $\langle v\sigma \rangle$ as a function of energy for 15-MeV C^{3+}. The data are compared to distorted-wave calculations of Griffin *et al.* (Ref. 9). — — —, 0 V/cm; —·—·—·, 2 V/cm; and ——, 5 V/cm.

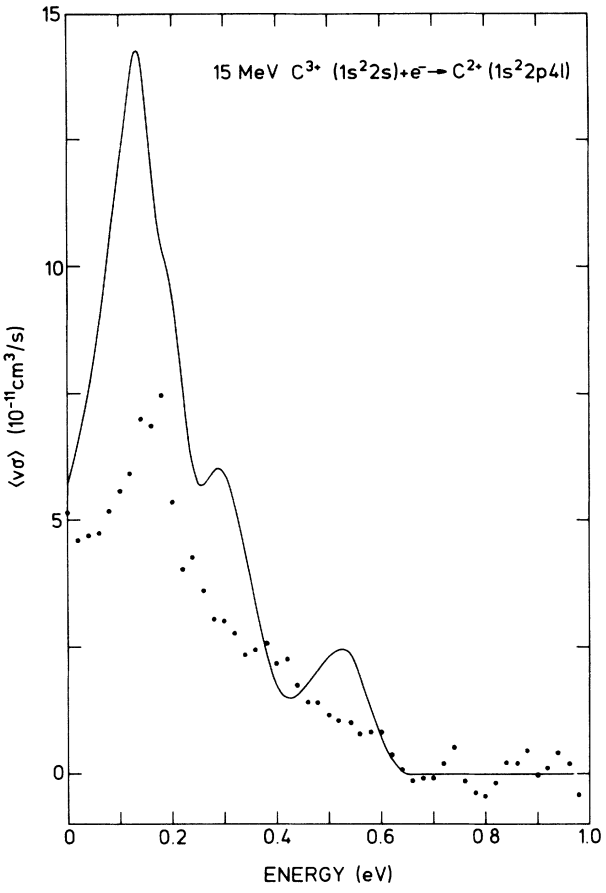

FIG. 14. DR spectrum for 15-MeV C^{3+} for relative energies between 0 and 1 eV. The DR resonance is due to the $1s^2 2s \rightarrow 1s^2 2p4l$ transitions. The solid line is the distorted-wave theory of Griffin *et al.* (Ref. 9).

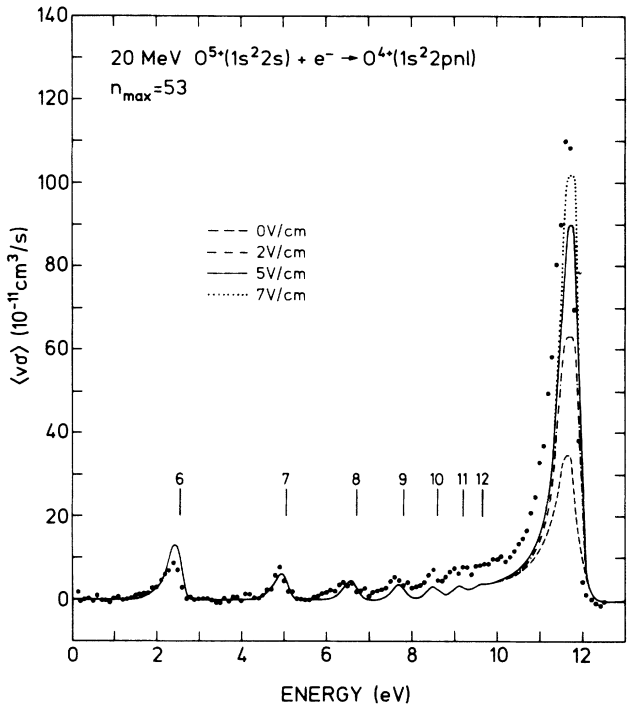

FIG. 15. Dielectronic-recombination rate coefficient $\langle v\sigma \rangle$ as a function of energy for 20-MeV O^{5+}. The data are compared to distorted-wave calculations of Griffin *et al.* (Ref. 9). — — —, 0 V/cm; —·—·—·, 2 V/cm; ——, 5 V/cm; and . . . ., 7 V/cm.

was displaced by 1 mm, we estimate the mean electric field to be in the order of 5 V/cm. Theory and experiment is then in better agreement. The disagreement at around $n=12$ between the experiment and theory, however, persists even for fields in the order of 7 V/cm. Previous measurements with O^{5+} also indicate that the theory underestimates the cross section.[6]

The data for the Li-like ions were deliberately not compared to calculations which were performed in a pure LS coupling[10] since this coupling scheme is known to yield cross sections which are a factor of two-thirds too low.[7]

IV. CONCLUSION

We have presented experimental data on dielectronic recombination with He- ad Li-like ions of C and O. A fitting procedure was employed to obtain the electron-velocity distribution. Very low "temperatures" were found: $kT_{\parallel}=10^{-3}$ eV and $kT_{\perp}=0.135$ eV. The Li-like C^{3+} and O^{5+} DR spectra have been compared with recent distorted-wave calculations. For C^{3+}, the experimental data and theory were generally in agreement for electric fields of 3 V/cm in the interaction region. An exception was the resonance with $n=4$, where the disagreement was about a factor of 2. For the same electric field strength, it seemed evident that theory underestimates the cross section for capture to high n states for Li-like O^{5+}. For the He-like ions, we found very large DR cross sections, in the order of 10^{-15} to 10^{-14} cm^2. It has been pointed out that the data exhibit structures which may indicate that configuration interaction is important for these ions.

ACKNOWLEDGMENTS

This work was supported by the Danish National Council of Sciences, the Carlsberg Foundation, and Ib Henriksen's Foundation. We wish to thank P. Hvelplund and H. Knudsen for many valuable discussions and support.

[1] M. Stobbe, Ann. Phys. **7**, 661 (1939).

[2] H. Bethe and E. Salpeter, *Quantum Mechanics of One- and Two-Electron Systems*, in Vol. 35 of *Handbuch der Physik* (Springer, Heidelberg, 1957), p. 88.

[3] J. Stevefelt, J. Boulmer, and J.-F. Delpech, Phys. Rev. A **12**, 1246 (1975).

[4] L. H. Andersen, H. Knudsen, P. Hvelplund, and P. Kvistgaard, Phys. Rev. Lett. **62**, 2656 (1989).

[5]P. F. Dittner *et al.*, Phys. Rev. Lett. **51**, 31 (1983).
[6]P. F. Dittner, S. Datz, P. D. Miller, P. Pepmiller, and C. M. Fou, Phys. Rev. A **35**, 3668 (1987).
[7]D. C. Griffin, M. S. Pindzola, and C. Bottcher, Phys. Rev. A **31**, 568 (1985).
[8]D. C. Griffin, M. S. Pindzola, and C. Bottcher, Phys. Rev. A **33**, 3124 (1986).
[9]D. C. Griffin, M. S. Pindzola, and P. Krylstedt, Phys. Rev. A **40**, 6699 (1989).
[10]D. J. McLaughlin and Yukap Hahn Phys. Rev. A **27**, 1389 (1983).
[11]D. J. McLaughlin and Yukap Hahn, Phys. Rev. A **29**, 712 (1984).
[12]P. F. Dittner, S. Datz, P. D. Miller, P. L. Pepmiller, and C. M. Fou, Phys. Rev. A **33**, 124 (1986).
[13]G. I. Budker *et al.*, Part. Accel. **7**, 197 (1976).
[14]R. Stensgaard, Phys. Scr. T **22**, 315 (1988).
[15]F. Brouillard, in *Atomic and Molecular Processes in Controlled Thermonuclear Fusion,* edited by C. J. Jochain and D. E. Post (Plenum, New York, 1983).
[16]J. R. Pierce, in *The Theory and Design of Electron Beams* (Van Nostrand, New York, 1954).
[17]M. Terasawa, T. J. Gray, S. Hagmann, J. Hall, J. Newcomb, P. Pepmiller, and P. Richard, Phys. Rev. A **27**, 2868 (1983).
[18]J. Newcomb, T. R. Dillingham, J. Hall, S. L. Varghese, P. L. Pepmiller, and P. Richard, Phys. Rev. A **29**, 82 (1984).
[19]G. W. Drake, Can. J. Phys. **66**, 586 (1988).
[20]Yukap Hahn and R. Bellantone (private communication).
[21]N. R. Badnell, M. S. Pindzola, and D. C. Griffin (private communication).
[22]K. Taulbjerg and J. Macek, Phys. Rev. Lett. **62**, 2766 (1989).
[23]R. D. Cowan and D. C. Griffin, Phys. Rev. A **36**, 26 (1987).
[24]A. Müller *et al.*, Phys. Rev. A **36**, 599 (1987).